

The Enhanced NOAA Global Land Dataset from the Advanced Very High Resolution Radiometer

Garik Gutman,* Dan Tarpley,*
Aleksandr Ignatov,*
and Steve Olson†

Abstract

Global mapped data of reflected radiation in the visible ($0.63\ \mu\text{m}$) and near-infrared ($0.85\ \mu\text{m}$) wavebands of the Advanced Very High Resolution Radiometer (AVHRR) onboard National Oceanic and Atmospheric Administration satellites have been collected as the global vegetation index (GVI) dataset since 1982. Its primary objective has been vegetation studies (hence its title) using the normalized difference vegetation index (NDVI) calculated from the visible and near-IR data. The second-generation GVI, which started in April 1985, has also included brightness temperatures in the thermal IR (11 and $12\ \mu\text{m}$) and the associated observation–illumination geometry. This multiyear, multispectral, multisatellite dataset is a unique tool for global land studies. At the same time, it raises challenging remote sensing and data management problems with respect to uniformity in time, enhancement of signal-to-noise ratio, retrieval of geophysical parameters from satellite radiances, and large data volumes. The authors explored a four-level generic structure for processing AVHRR data—the first two levels being remote sensing oriented and the other two directed at environmental studies—and will describe the present status of each level. The uniformity of GVI data was improved by applying an updated calibration, and noise was reduced by applying a more accurate cloud-screening procedure. In addition to the enhanced weekly data (recalibrated with appended quality/cloud flags), the available land environmental products include monthly 0.15° -resolution global maps of top-of-the-atmosphere visible and near-IR reflectances, NDVI, brightness temperatures, and a precipitable water index for April 1985–September 1994. For the first time, a 5-yr monthly climatology (means and standard deviations) of each quantity was produced. These products show strong potential for detecting and analyzing large-scale spatial and seasonal land variability. The data can also be used for educational purposes to illustrate the annual global dynamics of vegetation cover, albedo, temperature, and water vapor. Development of the GVI data product contributes to the activities of the International Geosphere–Biosphere Programme and Global Energy and Water Cycle Experiment and, in particular, to the International Satellite Land Surface Climatology Project. Monthly standardized anomalies of the GVI variables have been calculated for April 1985–present and are routinely produced on UNIX worksta-

tions, thus providing a prototype land monitoring system. Standardized anomalies clearly indicate that strong signals at the land surface, such as droughts and floods and their teleconnections with such global environmental phenomena as El Niño–Southern Oscillation, can be detected and analyzed. The monitoring of relatively small year-to-year variability is, however, contingent on the removal of residual trends/noise in GVI data, which are of the order of the analyzed effects.

1. Introduction

Climate studies require long-term sets of geographically referenced global land surface data to initialize and validate numerical models for the analysis of complex interactions and feedbacks within the earth system (IGBP 1992). Conventional ground observations cannot provide all the required information and must be supplemented from satellites. Another application of long-term global time series of satellite data is establishing climatologies of both top-of-the-atmosphere radiances and derived surface characteristics, which could in turn be used as a baseline for monitoring climate-scale variability. Among the objectives of the International Geosphere–Biosphere Programme (IGBP), the Global Energy and Water Cycle Experiment (GEWEX) and, in particular, the International Satellite Land Surface Climatology Project (ISLSCP) is aggregation of long-term global datasets that will provide a better insight into land–atmosphere interaction on diverse scales.

The Advanced Very High Resolution Radiometer (AVHRR) onboard National Oceanic and Atmospheric Administration (NOAA) satellites is most appropriate for the above applications due to the availability of spectral information for vegetation studies, operational global daily coverage, and the long-term continuous observational period. Additionally, AVHRR data are readily available at a nominal cost, whereas the high-resolution data from LANDSAT (land remote sensing satellite system) and SPOT (Système Probatoire d'Observation de la Terre) are costly and cover only limited regions of the globe episodically.

*Satellite Research Laboratory, NOAA/NESDIS, Washington, D.C.

†Research and Data Systems Corporation, Greenbelt, Maryland.

Corresponding author address: Garik Gutman, Satellite Research Laboratory, NOAA/NESDIS/ERA12, World Weather Building, Rm. 712, Washington, DC 20233.

In final form 20 December 1994.

©1995 American Meteorological Society

Over 13 yr of global AVHRR data have been archived at NOAA. Processing these data is a challenge for computational facilities, with navigation and mapping of the original data into a regular grid being the most computer-intensive tasks. The huge volumes of satellite data require compression in space and time. Two global-mapped AVHRR datasets over land have been aggregated by sampling those observations and mapping them into a regular grid, with further reduction of the data volume by temporal compositing that also reduces cloud contamination. They are the National Aeronautics and Space Administration (NASA) Global Inventory Monitoring and Modelling Studies (GIMMS) and the NOAA global vegetation index (GVI). Both are sampled AVHRR global area coverage (GAC) data, mapped into regular grids, with each map cell being represented by a single GAC 4-km pixel. The GIMMS dataset, with a spatial resolution of about $(8\text{ km})^2$, was produced on a continent-by-continent rather than globally uniform basis and does not include all AVHRR channels (IGBP 1992). Although no complete documentation, such as a user's guide, is available, this research dataset has been very useful for numerous studies (e.g., Tucker et al. 1985; Justice et al. 1985; Tucker et al. 1991; Los et al. 1994; among others).

The NOAA GVI, produced on a globally uniform basis with a $(0.15^\circ)^2$ resolution, is currently the most complete and documented global AVHRR dataset (IGBP 1992; Tarpley 1991; Goward et al. 1993; Gutman 1994a; Kidwell 1994). It has been primarily directed at studies of global vegetation distribution and dynamics—hence its title. Between 1982 and April 1985, measurements in only solar wavebands of AVHRR and their combination—normalized difference vegetation index (NDVI)—were archived as the first-generation GVI product. Many vegetation studies have been based on NDVI data (e.g., Malingreau 1986; Gallo and Flesch 1989; Kogan 1990; Tateishi and Kajiwara 1991; Hastings and Di 1994). Since April 1985, measurements in thermal IR wavebands and the associated solar zenith and satellite scan angles were added to the GVI dataset, forming the second-generation GVI product. This additional information made the GVI a unique tool for global land studies, although a number of challenging remote sensing and data management issues still needed to be properly addressed.

In 1989, analysis and reprocessing of the GVI dataset became a core project of the NOAA Climate and Global Change Program. The goal of the GVI project was to analyze and improve the GVI dataset to make it more useful for climate change-related applications; the present paper summarizes its accomplishments. A generic processing scheme for AVHRR data over land was worked out. Uniformity of

GVI data in time was improved by applying an updated AVHRR calibration and by reducing noise with better cloud screening. The following climate-related GVI products are currently available: monthly 0.15° global maps of the top-of-the-atmosphere reflectances, NDVI, brightness temperatures, a precipitable water index, and associated 5-yr climatologies (means and standard deviations). These variables and their monthly standardized anomalies are available starting with April 1985. All these data products show potential for investigation of large-scale land surface variability and for detecting environmental events, such as droughts and floods, that strongly affect vegetation development. The monitoring of moderate year-to-year surface variability requires further suppression of noise, enhancement of the signal, and removal of residual trends in data.

The experience, gained from work with the GVI data, is instrumental in creating and processing new generation 8-km Pathfinder (Ohring and Dodge 1992; James and Kalluri 1994) and 1-km IGBP (IGBP 1992) AVHRR datasets. Until these new and superior datasets replace it in the future, the GVI retains importance for both remote sensing and environmental scientists because of easy access to the original AVHRR radiances in four channels with associated viewing-illumination geometry and the new data products described herein.

The information content of AVHRR measurements over land is discussed in section 2. An overview of the basic steps in data processing is given in section 3. Section 4 concerns different aspects of land monitoring. Section 5 describes the present status of the GVI data products, including a prototype system for global operational land monitoring, and discusses remaining uncertainties and potential enhancements. Conclusions are given in section 6.

2. Information content of AVHRR measurements over land

The AVHRR is flown onboard the NOAA polar-orbiting satellites, the first of which was launched in 1978. These satellites are nearly sun-synchronous, flying at the altitude of about 850 km. With each pass, data are collected in a cross-track scanning mode along a swath about 2700 km wide, covering a range of viewing angles up to 56° . Each 24 h, global coverage consisting of 14.1 orbits is achieved, with one look during the daytime and one during the night. Under normal conditions, NOAA operates two polar orbiters, one in the morning and one in the afternoon. The second-generation GVI contains data from daytime

orbits of the afternoon satellites *NOAA-9* (April 1985–November 1988) and *NOAA-11* (November 1988–September 1994). These satellites cross the equator between 1400 and 1700 local solar time, with the equator crossing time drifting to a later hour as the satellite ages (Price 1991). Satellite orbit drift results in a systematic change of illumination conditions and local time of observation—one of the main sources of nonuniformity in multiannual satellite time series.

The AVHRR has five channels in the visible, near-infrared, and thermal infrared (IR) regions of spectrum: channels 1 (0.58–0.68 μm), 2 (0.73–1.0 μm), 3 (3.6–3.9 μm), 4 (10.3–11.3 μm), and 5 (11.5–12.5 μm). All these channels have been chosen within the relatively transparent atmospheric windows to allow observations of the surface. The first two channels measure solar-reflected light, whereas the land–atmosphere Planck emittance dominates in the thermal IR channels 4 and 5. Channel 3 is the most complicated case since both emitted and reflected solar components are comparable in this waveband. That was one of the reasons, in addition to frequent noisiness, for excluding channel 3 from the GVI dataset, and therefore, analysis of its information content is not given here. A brief review below discusses the information content of AVHRR measurements over land in cloud-free conditions. In studying the land surface, clouds should be excluded from the data since they obscure the signal from the surface in AVHRR wavebands.

a. Solar channels (channels 1 and 2)

1) SURFACE REFLECTANCE

The surface reflectance is characterized by the bidirectional reflectance distribution function (BRDF)—reflectance as a function of the observation–illumination geometry (e.g., Pinty and Verstraete 1992; Roujean et al. 1992; Cihlar et al. 1994). BRDF depends on the type of soil/vegetation and surface topography. If the BRDF is known, one can integrate it hemispherically to estimate the hemispherical spectral surface albedo for a particular band, but the limited range of AVHRR viewing geometry complicates derivation of the hemispherical albedo. Semiempirical relationships (e.g., Laszlo et al. 1988) can be used to convert spectral albedos into an integral over the full spectral domain—the broadband albedo, needed as an input to some numerical climate models.

2) VEGETATION INDEX

Availability of the 0.73–1.0- μm band makes AVHRR most attractive in studying processes at the biosphere–atmosphere interface. In this channel, the surface reflectance sharply increases for green vegetated surfaces as compared to soil/senescent vegetation. In channel 1, the presence of chlorophyll in green veg-

etation reduces the observed radiances (see, e.g., Curran 1980). Combining the AVHRR solar channels, Ch1 (channel 1) and Ch2 (channel 2), allows one to enhance the contrast between green vegetation and soil/senescent vegetation. The most widely used combination is the NDVI, calculated as $\text{NDVI} = (\text{Ch2} - \text{Ch1})/(\text{Ch2} + \text{Ch1})$. This particular combination was first proposed by Rouse et al. (1973) (not specifically for AVHRR) and has proved to be very useful because it partially compensates for changing illumination conditions, surface slope, and viewing aspect—factors that strongly affect observed radiances. The NDVI as a preferred index for monitoring vegetation was reenforced by an analysis of different spectral indices (Tucker 1979). Since the early 1980s, top-of-the-atmosphere NDVI derived from AVHRR has been used extensively for mapping vegetation on the continental and global scales (e.g., Tarpley et al. 1984; Tucker et al. 1985).

There is, however, an ambiguity in what NDVI measures, which stems from the unresolved combination of the amount and state of the vegetation in the radiometer field of view (Curran 1980). Usually, these two quantities are correlated since development of vegetation is associated with the increase of both chlorophyll amount and area coverage by the vegetation. The NDVI signal, however, saturates before other measures of vegetation amount, such as leaf area index (LAI) (e.g., Carlson et al. 1990). In any event, because of strong seasonal and spatial signals, this “simple” index of vegetation has been used extensively by the research community for more than a decade. In addition to analyzing vegetation distribution, monitoring its seasonal and interannual variability, and relating it to ecological variables (e.g., Malingreau 1986; Cihlar et al. 1991), it has also been suggested that NDVI be used in numerical models (see review by Gutman 1990) for estimating the ratio of actual to potential evapotranspiration (Mintz and Walker 1990), the ratio of soil heat flux to net radiation (Kustas et al. 1994), canopy resistance and photosynthesis (Sellers 1985), and green vegetation fraction and LAI (Carlson et al. 1990; Price 1990) [i.e., geophysical parameters identified by GEWEX (Global Energy and Water Cycle Experiment) as important for studying the land surface energy and water budget].

3) ATMOSPHERIC EFFECT

The reflectances in AVHRR channels 1 and 2, ρ_1 and ρ_2 , are affected by scattering/absorption processes in the atmosphere. The scattering is by molecules and aerosols (that may also absorb). Gaseous absorption is due to ozone in channel 1 and to water vapor in channel 2. Atmospheric effects are coupled in a complicated manner with surface BRDF. Thus,

derivation of the surface albedo and surface vegetation index from satellite measurements require atmospheric corrections, discussed in detail by Tanré et al. (1992) and Arino et al. (1992).

b. Thermal IR (channels 4 and 5)

The brightness temperatures in AVHRR channels 4 and 5, T_4 and T_5 (K), depend mainly upon the surface temperature, total-column atmospheric water vapor, and surface-atmosphere temperature gradient, so that the former two parameters can be estimated using split-window techniques (see, e.g., Dalu 1986; Kerr et al. 1992; Prata 1993).

1) LAND SURFACE TEMPERATURE

A useful piece of information for surface characterization is land surface temperature (LST). However, there is some ambiguity in its definition because of the complex character of the land surface—its heterogeneity, roughness, and multilevel vegetation (e.g., Li and Becker 1993). The split-window technique for LST retrieval usually is based on a linear combination of T_4 and T_5 . The accuracy of the estimated LST is restricted mainly by the effect of unknown and spectrally variable emissivity, which is a function of soil/vegetation type, topography, and observation geometry (Prata 1993).

2) PRECIPITABLE WATER INDEX

Dalu's (1986) theoretical considerations show that under certain assumptions total-column atmospheric water vapor amount (total precipitable water) can be derived over the ocean in clear conditions using the difference between the two AVHRR brightness temperatures. A precipitable water index (PWI) can thus be introduced as $PWI = T_4 - T_5$. Recent investigations analyze the potential and limitations of using PWI to estimate water vapor amount over land (Justice et al. 1991; Eck and Holben 1994). Variable aerosols, surface emissivity, and surface-atmosphere temperature gradients are the major factors affecting the relationship between PWI and the actual water vapor amount.

c. Combining solar and thermal IR channels

A combination of NDVI and LST was proposed as a method for assessing the surface moisture status and fractional vegetation cover over nonuniform land surfaces (Carlson et al. 1990; Price 1990; Nemani et al. 1993). The basic physical assumption is that the more heavily vegetated surfaces are associated with greater evapotranspiration and hence should be cooler than the less vegetated ones. Another reason that soil temperatures are higher than canopy foliage temperatures is the greater efficiency of the leaves at shedding absorbed energy (Choudhury 1989). Friedl and Davis (1994) indicate that in "well-watered" conditions the

proportion of the soil background in the radiometer field of view, rather than evapotranspiration, explains the observed NDVI–LST negative correlation.

3. Generic processing of AVHRR data

This section and section 4 are pertinent to AVHRR data use in general and the GVI dataset in particular. The present section proposes an "ideal" processing scheme, which indicates the data flow and production, based on our experience with the GVI project. It should not be confused with the present accomplishments of the GVI project described in section 5. Although the introduction of a new structure in this review paper may appear as a complication, the lack of consensus on processing and nomenclature motivated us to present our views on these important issues here. The structure, given below, facilitates general overviewing of the main levels in data production and evaluating the present status of the GVI data products, as well as those within other projects.

Data for climate studies are usually subdivided into three general levels: A) primary instrument readings; B) retrieved geophysical parameters after appropriate quality assurance; and C) fields prepared from level B data. Our experience with GVI data suggests that one more level, D level, should be added to distinguish between generating complete fields and their statistical analysis. The currently proposed structure complies with the above categorization as well as with the data nomenclature in the International Satellite Cloud Climatology Project (Rossow and Schiffer 1991).

a. The A level

This level involves preprocessing of the acquired satellite sensor readings. It is described in detail by NOAA's documentation, such as the NOAA *Polar Orbiter Data User's Guide* (Kidwell 1995), and therefore is not addressed here.

b. The B level

This level includes calibration and radiometric corrections of the A-level data; identification of the pixels that can be used for land studies; and transformation of the bidirectional reflectances, ρ_1 and ρ_2 , and brightness temperatures, T_4 and T_5 , into climate-related land variables (surface albedo and temperature, fraction of vegetation, LAI, photosynthetically active radiation, etc.). The B-level data are mostly remote sensing oriented. They include auxiliary information, such as observation–illumination geometry, calibration coefficients, quality/cloud (QC) flags, that allow tests and development of methods to improve the quality of data products.

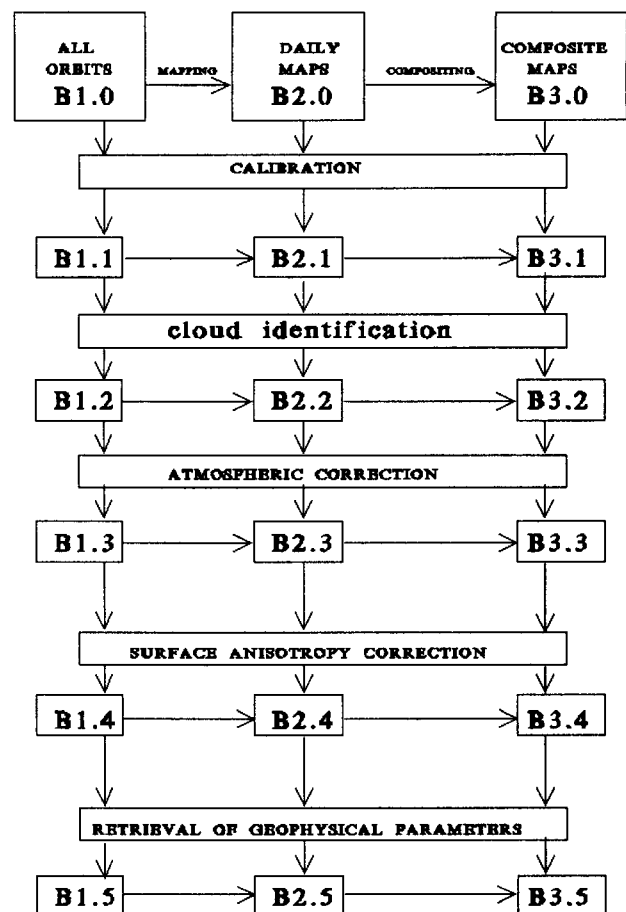
Steps in the B-level processing are shown in Fig. 1. The AVHRR data are supplied with information on navigation and prelaunch calibration appended but not applied, and are usually referred to as the NOAA 1B level—B1 in our notation. The data mapped daily into a regular geographical grid are denoted as B2. Temporal sampling is usually done by compositing procedures. The composite maps are referred to as B3. This step provides users with BX.0 data ($X = 1, 2, 3$): B1.0 (orbits), B2.0 (daily maps), B3.0 (composite maps). Any of them may be used as a starting point for further processing. The BX.0 data contain original raw counts in AVHRR channels and information on calibration, navigation, and observation–illumination geometry.

The first step of B-level data processing involves calibration—conversion of sensor counts to physical quantities (ρ_1, ρ_2, T_a, T_s)—leading to BX.1 data products. At the next step, BX.2, quality/cloud identification of each pixel is done, with the results of different tests being packed in QC flags. The generated QC maps are appended to BX.1, making it the BX.2 data. Corrections for atmosphere and surface anisotropic and diurnal variabilities are made at the next two steps, BX.3 and BX.4, respectively. Transformation to land surface parameters is carried out at the final step BX.5. The last three steps are made by means of look-up tables so that the whole image, independent of QC flags, is transformed with efficient use of computer time. At the next level, it is decided which pixels are to be retained for land studies. Note that most of the boxes have two arrows coming in and two coming out, which implies that the processing sequence is nonunique and that the derived product (at each step) can be obtained in more than one way. The path that is used to derive the product thus should be added in a more detailed version of the proposed nomenclature.

To identify the time–space resolution of data products, we propose a flexible nomenclature: BX.Y/TS, where $X = 1, 2, 3$ and $Y = 1, 2, 3, 4, 5$ denote the stage and step of the B level at which the product was generated, and TS stands for the temporal and spatial resolutions, respectively. For example, T can be H, D, W, Dk, M, S, or Y for hourly, daily, weekly, dekadal, monthly, seasonal, and yearly, respectively. It is implied that at the B level the original dataset resolution is not degraded (e.g., $S = 1, 4, 8, 15$ standing for 1, 4, 8, and 15 km, respectively).

c. The C level

The data are for the users who need products for, for example, initialization and validation of models and do not want to spend time and resources on processing the remotely sensed data. At this level (Fig. 2), the B data are used as input, all auxiliary information is



between various parameters on different spatial/temporal scales, and other statistics. The D-level products are most useful for climate analysis. Combining the D- and C-level products can be used for monitoring purposes, as described below. The nomenclature introduced above is applicable to the D products as well.

4. Land-monitoring aspects

This section discusses the issues related to monitoring from AVHRR in general. Only some, but not all, of these aspects have been accounted for in the GVI data products at present. Some are still in a research and development stage. The present status of the GVI data production and the issues to be resolved are described in the next section.

a. Standardized anomalies

We define monitoring as detection of anomalies $\Delta = V - \langle V \rangle$, that is, deviations of the observed quantities V from their multiannual means $\langle V \rangle$. To quantitatively estimate the extent (reality and magnitude) of the anomalies, one has to have a reference noise level with which the anomalies should be compared (Malingreau 1986) and that is provided by the climatological variance around the mean σ^2 . Assessment of statistical significance of the anomalies as compared to the level of inherent local year-to-year fluctuations is done by considering standardized anomalies $\delta = \Delta/\sigma$. The above approach is hardly new and has been used in climate studies for decades. The lack of long-term satellite datasets has prevented this method from being widely used in remote sensing.

b. Multiparameter monitoring

AVHRR has five spectral bands, allowing retrieval of many land surface geophysical parameters. Although a comprehensive monitoring system should use all of them, usually only one monitoring parameter is used (e.g., NDVI), which fails to characterize the surface fully. In aggregating NDVI, individual information from solar channels is lost. Furthermore, the thermal IR channels provide additional information. For example, both droughts and floods are associated with lowered NDVI but have different IR signatures. Using several monitoring parameters derived from AVHRR reduces the ambiguity in interpretation of statistically significant anomalies.

c. Using top-of-atmosphere parameters

Monitoring of land surface implies the use of surface geophysical parameters, such as LAI or fraction of vegetation (i.e., CX.5 data in our nomenclature).

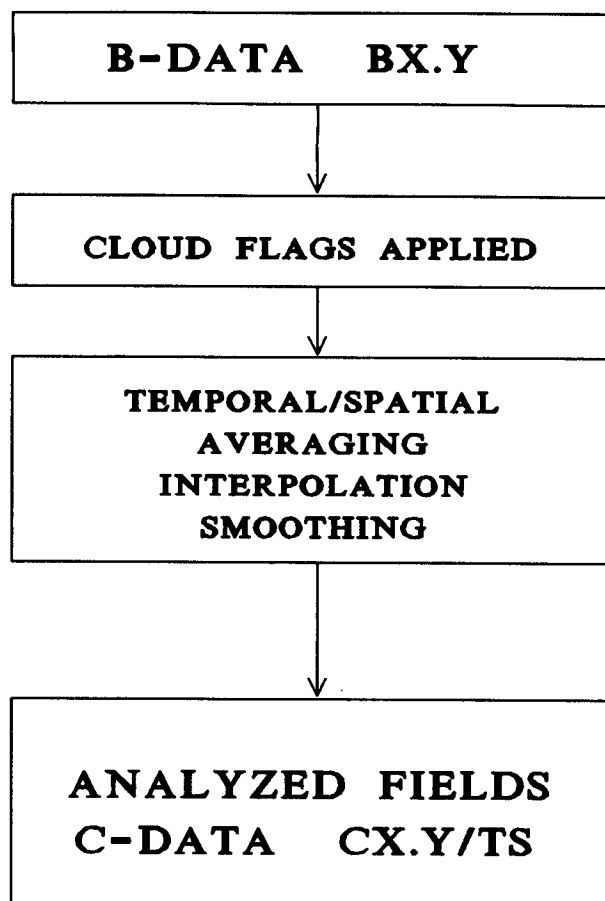


Fig. 2. The C level of the generic AVHRR processing scheme.

However, retrieval algorithms for surface parameters are not always available or reliable. An equivalent approach to monitoring can be based on the standardized anomalies of surface ρ_1 , ρ_2 , NDVI, T_4 , and T_5 normalized to a common observation–illumination geometry and time of day ($\delta_{CX.4}$). If the latter effects contribute negligibly to the variance of remote signal, then $\delta_{CX.3}$ may be used. If most year-to-year variability in the observed data comes from the surface (since atmospheric window regions are used and surface contribution is expected to dominate), even standardized anomalies of top-of-atmosphere (TOA) parameters ($\delta_{CX.2}$) can be used for most practical purposes. Screening of cloud contamination is, however, mandatory. The currently developed monitoring system within the GVI project, based on calibrated and cloud-screened TOA composite data (C3.2), is described in section 5d.

d. Limiting factors

The use of AVHRR for monitoring is seriously hampered because of the nonuniformity of the

satellite time series. This includes satellite/sensor discontinuities due to satellite/sensor change and trends caused by sensor instability (Kaufman and Holben 1993) and by satellite orbit drift (Price 1991). The AVHRR solar channels are not calibrated in flight and degrade with time, which is taken care of by applying postlaunch calibration (Rao and Chen 1994). The satellite-to-satellite change and orbital drift affect all variables because of changing illumination and diurnal surface/atmosphere variability. Large-scale atmospheric perturbations from volcanic eruptions like Mt. Pinatubo contribute to nonuniformity of time series because stratospheric aerosols produced by these eruptions have a strong and persistent impact on observed radiances, mostly in solar channels (Stowe et al. 1992). All the above factors present difficulties in using AVHRR data if atmospheric/angular corrections are not applied at the B level.

5. The present status of GVI data products

The GVI products that have been routinely available at NOAA are B2.0 (daily maps) and B3.0 (weekly composite maps). The work in the GVI project has been based on weekly composites (B3.0). The creation of the third-generation GVI consists of reprocessing the second-generation GVI dataset (April 1985–present) by the procedures described below and summarized in Fig. 3. Atmospheric, anisotropic, and diurnal variability corrections and derivation of surface geophysical characteristics (dashed box) are bypassed in the current work but remain the subject of further research and development. The data products that have recently become available in addition to B3.0 are B3.1/W15, B3.2/W15, C3.2/M15, and D3.2/M15.

a. GVI weekly products

(B3.1/W15 and B3.2/W15)

The counts in AVHRR thermal channels are converted to T_4 and T_5 (Kidwell 1991; Kidwell 1994) and corrected for calibration nonlinearity (Rao 1993). Reflectances in the solar chan-

nels ρ_1 and ρ_2 are calculated using the updated (Pathfinder) calibration (Rao and Chen 1994), which accounts for sensor degradation, and then corrected for sun–earth distance. The $NDVI = (\rho_2 - \rho_1)/(\rho_2 + \rho_1)$ and $PWI = (T_4 - T_5)$ are calculated at the B3.1 level to retain accuracy since all B3 product values are packed into eight bits.

Composite imagery in many parts of the world is often cloud contaminated and should be cloud screened before any geophysical analysis. The B3.2 cloud/clear identification technique uses T_4 thresholds dependent upon month, region, and viewing angle as described in detail by Gutman et al. (1994). Together with updated calibration, the generation of QC flags is the major enhancement to the second-generation GVI dataset. The B3.2 data products for the period April 1985–present include weekly composite maps of the TOA ρ_1 , ρ_2 , $NDVI$, T_4 , T_5 , PWI , the associated solar zenith and satellite scan angles, and QC flags. The relative azimuth angle (i.e., the difference between solar and satellite azimuth angles) needed for atmospheric/angular corrections is not supplied with the dataset as a separate file but is calculated within the reading program appended to the dataset. An example of a B3.2/W15 product—a weekly composite $NDVI$ map with a QC mask—is given in Gutman et al. (1994).

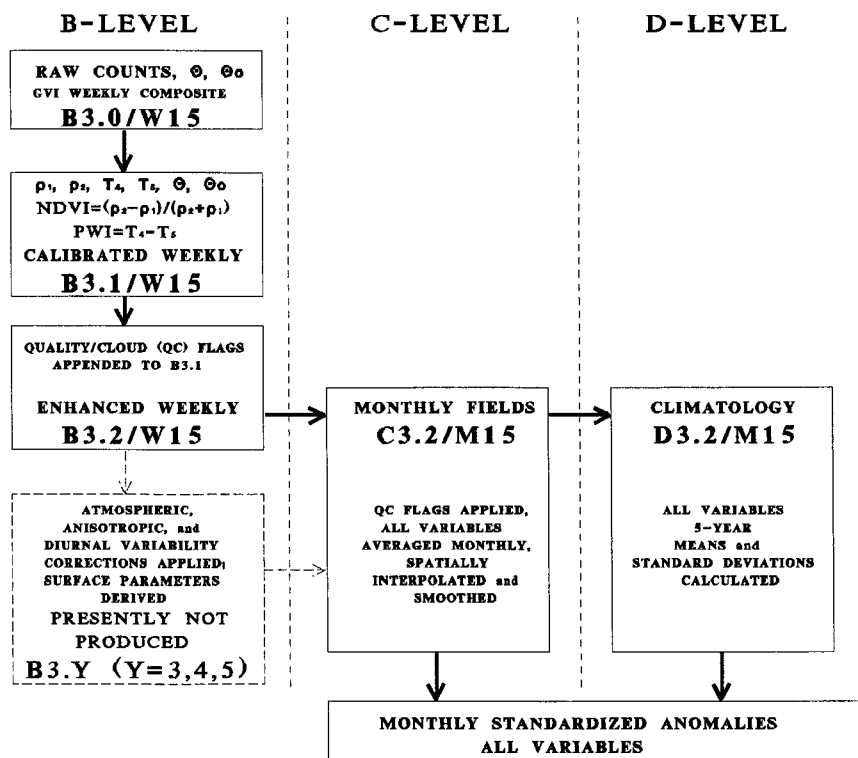


FIG. 3. A schematic summary of the procedures used for GVI data products.

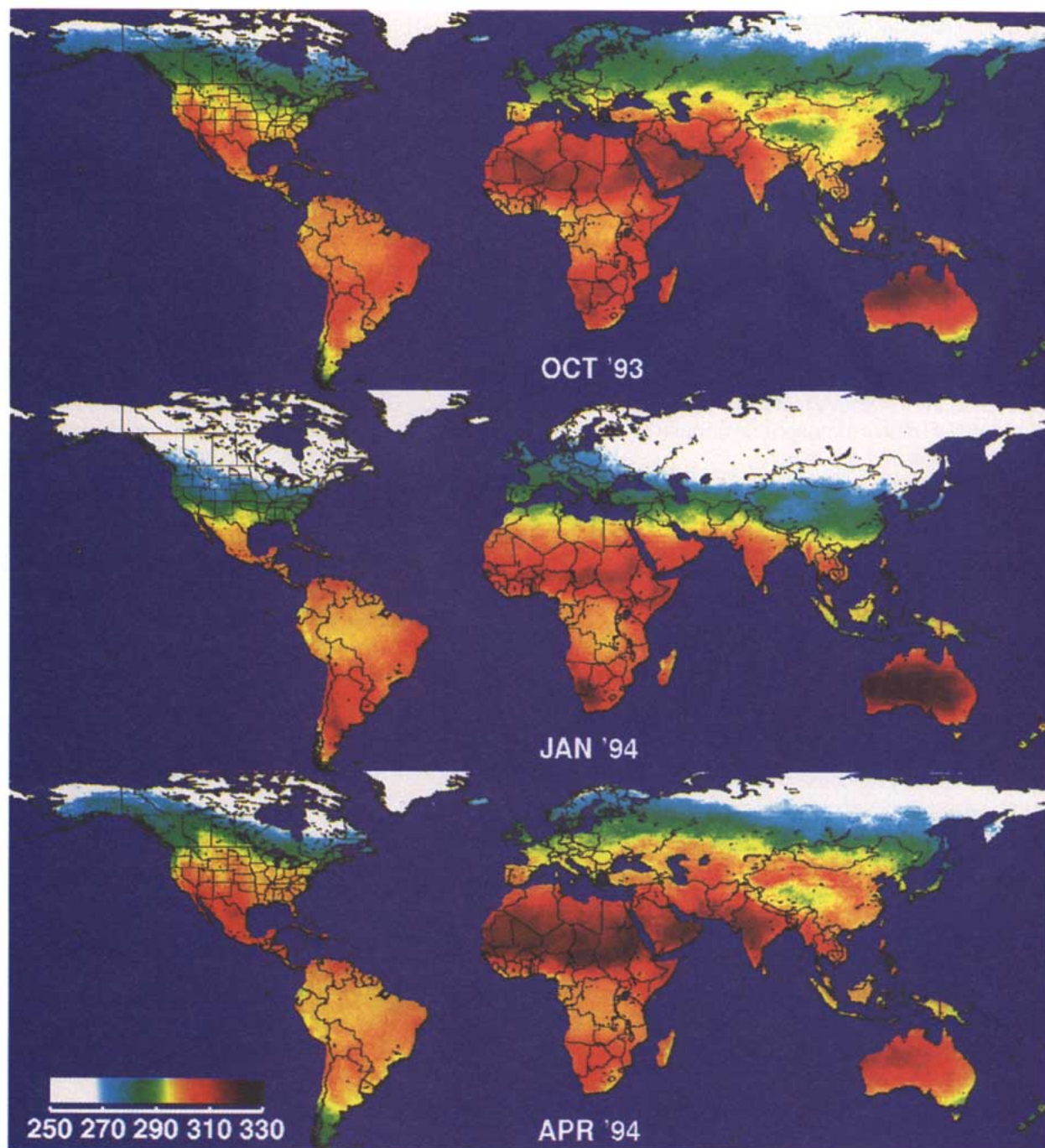


FIG. 4. Global monthly mean maps of T_4 (K): October 1993, January 1994, and April 1994.

b. GVI monthly products (C3.2/M15)

The C3.2/M15 production flow includes the following steps: 1) QC flags are applied on a weekly basis, resulting in data gaps; 2) each quantity is averaged over one month for each map cell to partially fill in the data gaps and reduce some of the angular variability (the number of cloud-free weeks is stored as an additional map); 3) bilinear spatial interpolation is

applied to the missing data areas with persistent cloudiness in monthly averaged images; 4) 3×3 map-cell smoothing is done to partially account for the imperfection of cloud screening, to filter out atmospheric and angular variabilities, and to compensate for random spatial sampling from GAC data into the GVI map cells. The above procedure yields monthly mean values for TOA ρ_1 , ρ_2 , NDVI, T_4 , T_5 , and PWI at

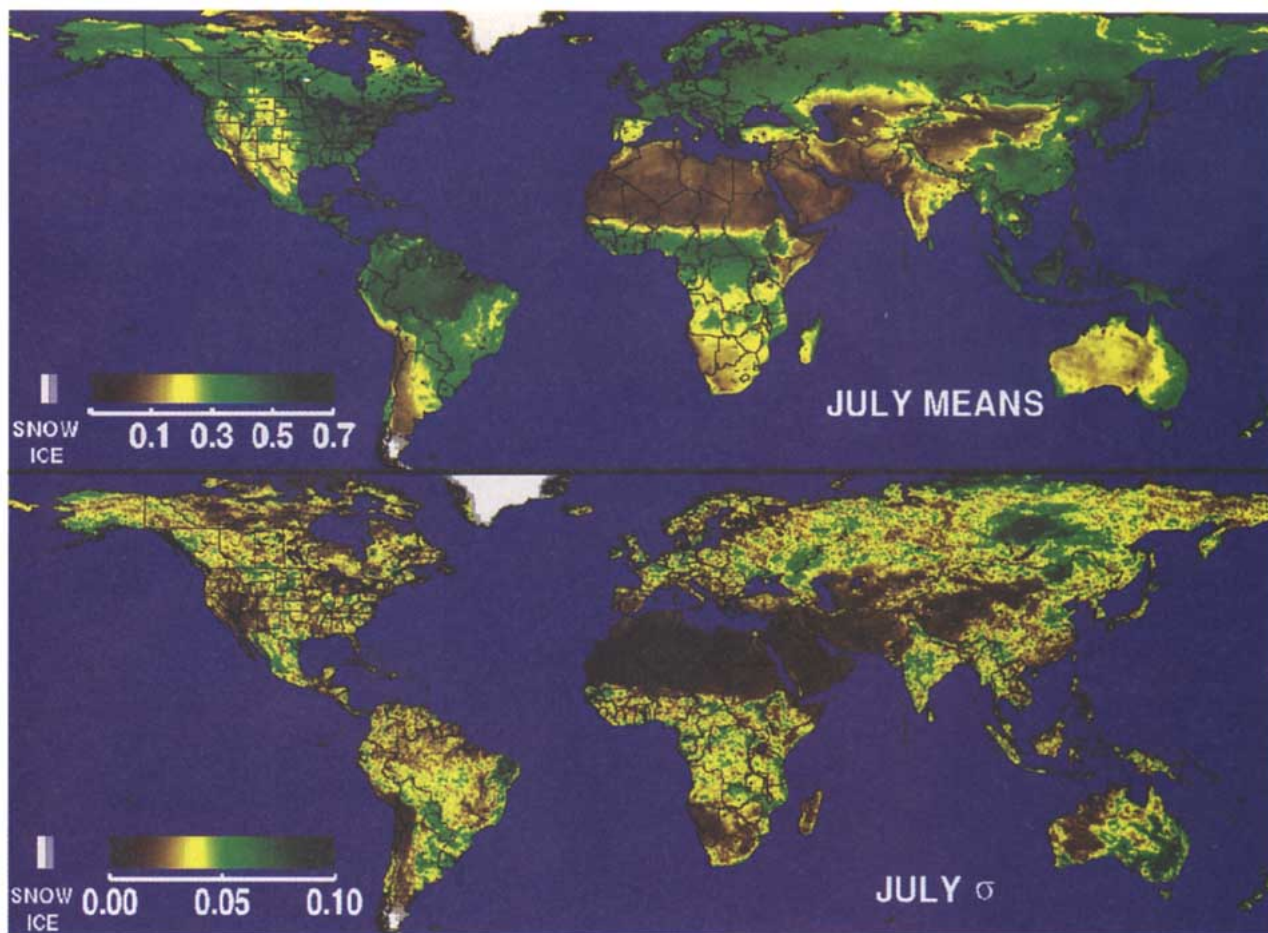


FIG. 5. Global NDVI 5-yr July climatology: means (top) and standard deviations (bottom).

each GVI map cell for each month of each year. Figure 4 shows examples of C3.2/M15 products: global monthly maps of T_4 for October 1993, January 1994, and April 1994. The T_4 map represents near maximum rather than daily mean brightness temperature because of spacecraft midafternoon observation time.

c. GVI monthly climatology (D3.2/M15)

A 5-yr climatology of means and variances at 0.15° resolution (D3.2/M15) has been developed from the C3.2/M15 monthly fields of TOA ρ_1 , ρ_2 , NDVI, T_4 , T_5 , and PWI using data from April 1985 to December 1987 (NOAA-9), and from January 1989 to March 1991 (NOAA-11). The NOAA-9 data for 1988 and most of 1991 onward (after the Mt. Pinatubo eruption) were excluded since no angular/atmospheric corrections were applied.

Global maps of multiannual means and standard deviations of clear-sky AVHRR-derived variables have been generated for the first time under the GVI project, although global 3-yr NDVI statistics have been avail-

able during the past year (Hastings and Di 1994). Figure 5 shows the NDVI 5-yr climatology for July. Despite the short 5-yr base period, the areas with high interannual vegetation variability are clearly depicted on the map of standard deviations and are of particular interest to climatologists. The areas in central Siberia, southeast Australia, and northeast Brazil show high interannual NDVI variability, the latter being attributed to droughts caused by El Niño–Southern Oscillation (ENSO) during the 5 yr. Figure 6 shows the completion of the annual cycle of the mean NDVI from Fig. 5. The areas in white ($T_4 < 270$ K) are classified as stable snow/ice and in gray ($270 \text{ K} < T_4 < 280 \text{ K}$) as transitional (unstable) snow/ice, both having $\rho_1 > 20\%$.

Figure 7 shows the July climatology of ρ_1 , T_4 , and PWI. The global and seasonal distribution of PWI agrees with the observed distribution of precipitable water (Tuller 1968). This suggests a potential for PWI as a measure of large-scale water vapor distribution over land (see section 2b). The multispectral GVI data can be used for deriving other land variables (e.g., LST

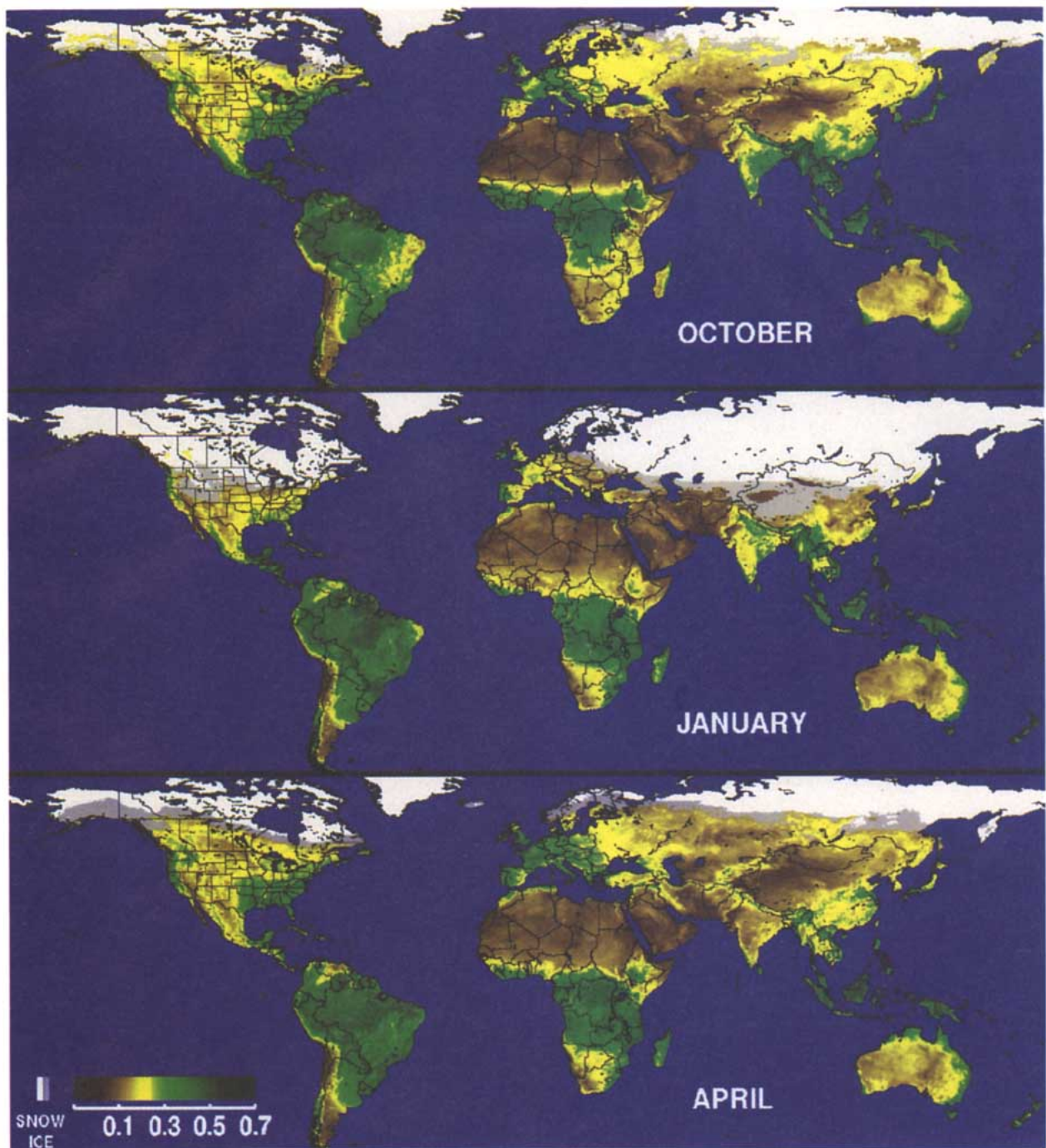


FIG. 6. Global NDVI 5-yr means for October, January, and April. The areas in white ($T_4 < 270$ K) are classified as stable snow/ice and in light gray ($270 \text{ K} < T_4 < 280 \text{ K}$) are classified as transitional (unstable) snow/ice, both having $p_1 > 20\%$.

and albedo) and for improving classifications of bioclimate based on temporal analysis of NDVI alone (e.g., Tucker et al. 1985; Townshend et al. 1987).

d. Prototype of a global land-monitoring system

A prototype global land monitoring system has been developed based on a Silicon Graphics UNIX

workstation. It is an evolving system, in which some parts can be improved and/or replaced, and is suitable for routine operations requiring very little human intervention.

Each week, composite B3.0 data are automatically accessed and copied to a UNIX workstation magnetic disc. The production of B3.1 and B3.2 follows (i.e.,

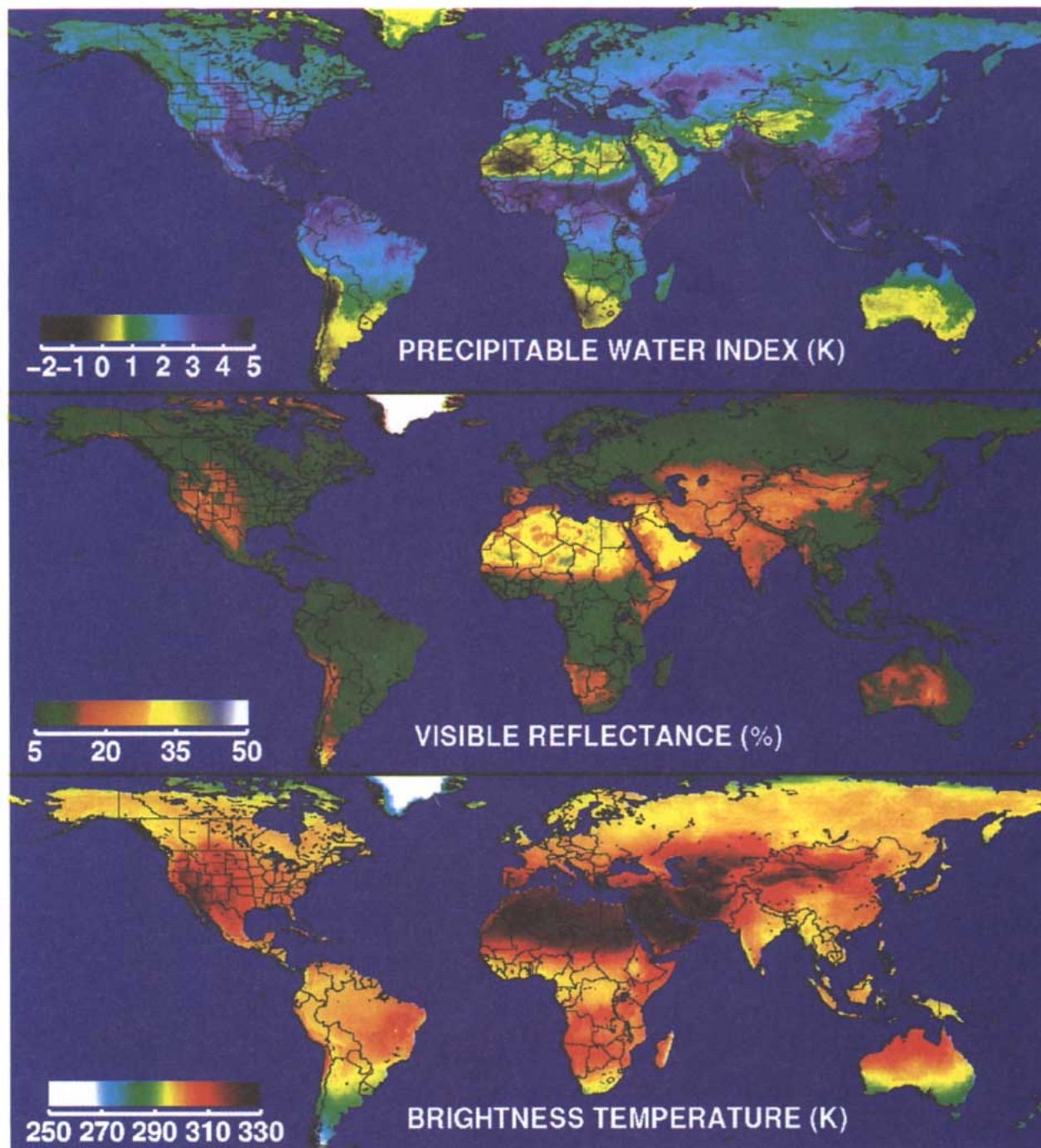


FIG. 7. Global 5-yr July means of p_1 , T_4 , and PWI.

calibration and generation of QC masks). The enhanced weekly product is then appended to the existing NOAA archive. At the beginning of each month, the previous five B3.2 weekly products are processed at the C level (i.e., the QC flags are applied and monthly averaging, interpolation, and smoothing are carried out). Then the monthly standardized

anomalies are generated and made available for climate analysis and interpretation. Display of the seasonal and year-to-year dynamics on a global scale of the derived land products is now possible by means of the animation loops on workstations using a menu-driven program and the Interactive Data Language software.

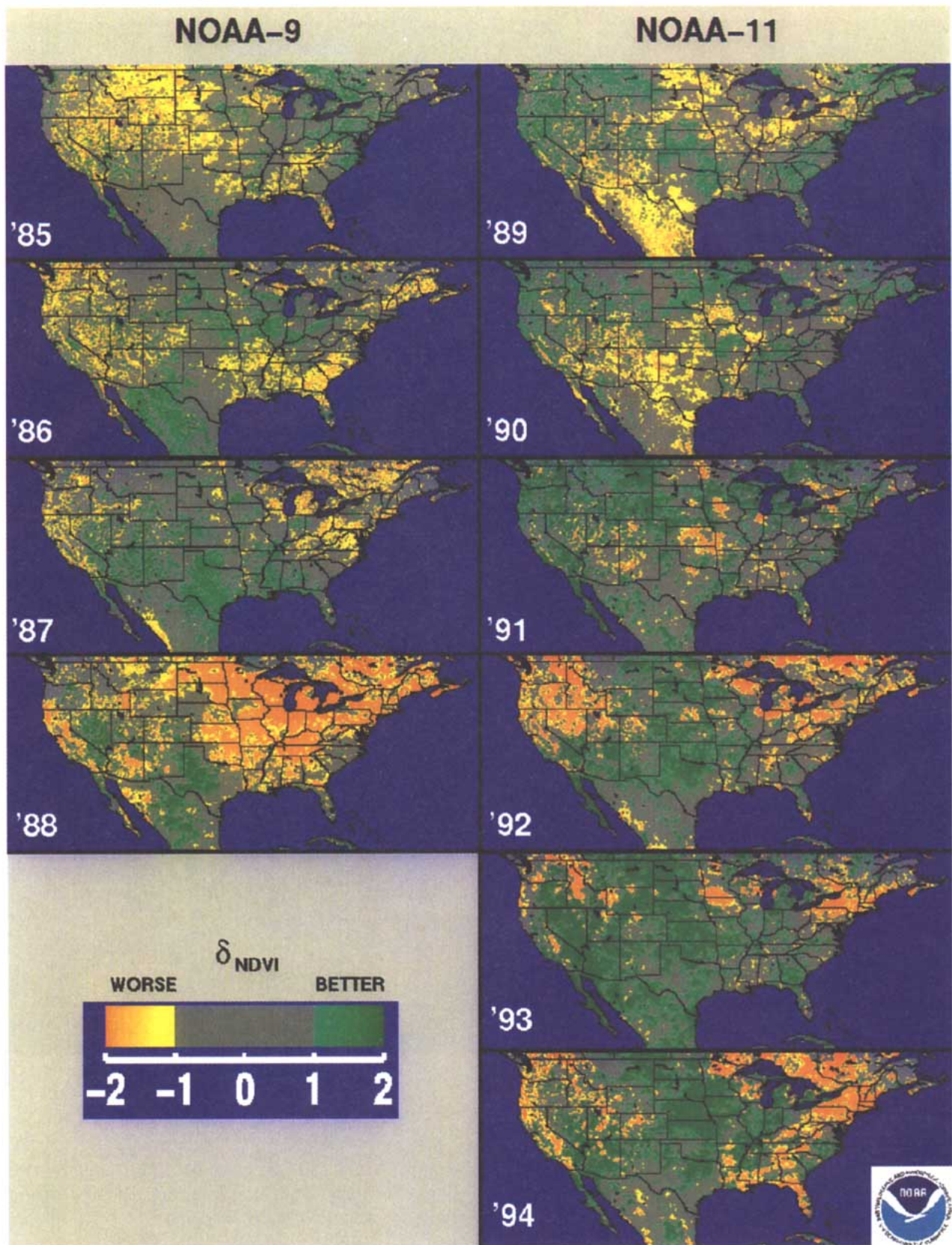


FIG. 8. Standardized anomalies of NDVI for the United States in July (1985–94), defined as departures from the 5-yr means divided by the 5-yr standard deviations.

An example of the standardized anomalies δ_{NDVI} for July over the United States during 1985–94 (Fig. 8) illustrates the multiannual potential of the GVI products. (Note that the positive and negative anomalies for the whole time series are not mutually balanced since the base period for climatology development includes only five of the nine presented years.) In general, the derived anomalies compare well with the maps of the Palmer drought index (PDI) produced by NOAA and the U.S. Department of Agriculture, except for some special situations. For example, the areas where the 5-yr mean NDVI estimates are biased are not easily interpreted, particularly in the west, where PDI indicates dry conditions during all 5 yr. During most of the NOAA-11 observational period, dry areas in the west also show a “greening” trend, which we attribute to residual calibration error and which seems to be partially compensated for by the sun-angle effect in 1994 (Gutman and Ignatov 1995). Further, note that both moisture deficit (droughts) and excess (floods) are associated with lowered NDVI. The “Great Flood” of 1993 in the area of Iowa and the flooding of 1994 in northern Florida appear as patterns of negative anomalies in Fig. 8. Additional information, such as thermal IR and/or microwave measurements should be used to distinguish insufficient from excessive moisture conditions. The derived temperature anomalies δ_{T_4} are affected by the diurnal variability of the observed brightness temperature as a result of satellite orbit drift (see section 4), which presents difficulties in monitoring AVHRR temperatures (Gutman and Ignatov 1995). Corrected temperature time series from AVHRR and/or data from other sensors should alleviate this problem.

e. Remaining uncertainties and potential enhancements

All of the processing levels have potential for improvement. The calibration and cloud screening should be refined. The B3.3–B3.5 products are yet to be generated. The use of optimal averaging and interpolation on the C level is preferable to fill in the data gaps. These, however, require the spatial/temporal correlation functions, which are not available now. The D level can be improved by using longer time series and developing other statistics.

1) ATMOSPHERIC, ANISOTROPIC, AND DIURNAL VARIABILITY EFFECTS

The major distortion of the signal in solar channels by the atmosphere is due to aerosol and water vapor. Global observations of these constituents are not readily available. Research is under way to derive this information from AVHRR data [e.g., using PWI for water vapor amount (Eck and Holben 1994)]. Much

effort has yet to be invested to correct data for stratospheric and tropospheric aerosol effects. Several studies have shown that much of the contribution to angular variability in the observed radiances is due to surface anisotropy (Roujean et al. 1992). Thus, even if the atmospheric corrections are made, it is unclear how the results could be interpreted. A single globally applicable correction is not possible due to the variability of surface effects in space and time. Models of only a few vegetation types are unlikely to be generic because of topography and mixture of vegetation types. Surface and atmospheric diurnal variability is most pronounced in the thermal data, resulting from satellite orbit drift. Normalization to common observation time is needed for monitoring interannual variability in surface temperature.

2) AN ALTERNATIVE APPROACH

Since atmospheric, anisotropic, and diurnal variability corrections of GVI data are currently infeasible, an alternative approach has been proposed for developing TOA regional empirical angular/diurnal variability functions (REAF) for each limited region of the global land surface for limited periods—for example, monthly (Gutman 1994a,b). (Note that diurnal variability can be expressed as sun-angle dependence for a given latitude; geostationary satellite data could be used for developing this dependence.) The number of the REAFs may be reduced using cluster analysis at a later stage. The REAFs are in turn used to normalize all data to a common sun–target–sensor geometry. Pilot studies indicate that the time series become more stable after TOA normalization (Gutman 1994b; Ba et al. 1995). The effective elimination of angular biases allows more reliable interpretation of the results and widens the area of applicability for analysis. The methodology has to be improved and tested further before its global development is undertaken.

3) LESSONS LEARNED

While analyzing the operational production of GVI (B3.0), a number of lessons about data collection have been learned. These lessons indicate how the AVHRR data management could be improved and have implications for the NOAA/NASA Pathfinder AVHRR land dataset. In the NOAA GVI operations, only afternoon satellite passes are collected, preventing diurnal variability studies on one hand and leading to persistent cloud contamination in some areas on the other hand. Data should be collected from each of the currently operating NOAA polar orbiters, allowing more coverage and opening new opportunities for research. Compositing in the NOAA GVI collection is currently done by using the maximum of a simple difference Ch2–Ch1, leading to a stronger bias in observation

geometry as compared to using maximum NDVI (Gutman 1991). Both (Ch2–Ch1) and NDVI compositing procedures are not appropriate for collecting clear observations over snow and desert regions. Other methods (e.g., using T_4) should be explored. The NDVI and Ch2–Ch1 compositing procedures retain cloud-contaminated data over water surfaces. Since negative values of NDVI (and Ch2–Ch1) are observed over cloud-free water, compositing by the absolute value would add information over water bodies in the composite imagery. Thus, compositing, if unavoidable, should be done using maximum absolute value NDVI or T_4 . Yet, methods other than compositing should be developed to reduce data volume, preferably after cloud screening has been done. Therefore, cloud/clear discrimination should be done on the original daily images so that only clear pixels are mapped. A 10-bit precision is recommended for thermal IR channels, which are currently truncated to 8-bit precision (i.e., 0.5 K) in the NOAA GVI. All channels should be collected. Channel 3 in the GVI dataset collection could facilitate discrimination of snow from clouds and detection of aerosols. Most of these recommendations are already in effect in the Pathfinder processing scheme and should be implemented in NOAA's operations.

6. Conclusions

An overview of research and development with the NOAA global vegetation index dataset under a core project of the NOAA Climate and Global Change Program has been given and the enhanced GVI data products described. All the products (B3.2/W15, C3.2/M15, and D3.2/M15) are available from NOAA archives. The D3.2/M15 will also be available on CD-ROM. The C3.2/M15 and D3.2/M15 products reside on a UNIX system at the National Environmental Satellite Data and Information Service and will be made available for browsing and animation. The latter can be used for educational purposes to illustrate the global annual dynamics of vegetation cover, albedo, temperature, and water vapor.

The newly derived C and D products can be easily accessed by climatologists for the analysis of inter- and intra-annual land climate variability, such as response of the surface state to ENSO episodes. Deeper involvement of climatologists in the data products analysis and their close interaction with the "data producers" is imperative at this stage. Given the improvement of the data quality, the present study suggests that there is more potential in this dataset

than previously thought (e.g., Thomas and Henderson-Sellers 1987), although it should be borne in mind that the remaining uncertainties limit this potential. The annual global distribution of the GVI variables is currently more reliable than the derived interannual variability, which is useful only when the surface change is relatively strong compared to the noise level. Further reduction of noise and removal of trends will increase the monitoring potential of AVHRR land data.

The operational production of monthly anomalies continues. The previous month's anomalies are available during the first week of the current month. Weekly monitoring for the areas with frequent cloud-free skies can be developed if more progress is achieved in angular/atmospheric corrections.

Despite the remaining uncertainties in the monthly GVI data products, their information content is higher than that of the GIMMS-derived $1^\circ \times 1^\circ$ NDVI monthly dataset (Los et al. 1994) because of finer spatial resolution, the availability of individual channel reflectances and temperatures, and more accurate cloud screening. The GVI dataset is unique in that it is global, multiseasonal, multispectral, and multiannual. These GVI features are useful not only for environmental studies and numerical modeling but also for further development of the remote sensing methodology and processing of the 8-km Pathfinder and 1-km IGBP AVHRR datasets. Both Pathfinder and the 1-km projects can use the GVI experience for generating C- and D-level products for the environmental research community. Development of the GVI data products contributes to the activities within IGBP, GEWEX, and, particularly, ISLSCP.

Acknowledgments. The GVI project has been supported by the NOAA Climate and Global Change Program. Without its continuous funding, the construction of the UNIX-based system for generating global AVHRR land data products would not have been possible. Critique and reviewing by the NOAA CGCP manager, Dr. A. Gruber, motivated this paper. D. Sullivan [Research Data Systems Corporation (RDC)] and J. Powers (NESDIS's Interactive Processing Branch) are acknowledged for the development of the processing and visualization system. Contributions in the project by M. Halpert and Dr. C. Ropelewski (NOAA Climate Analysis Center), and P. Schultz, R. Hucek, and L. Rukhovetz (RDC) are acknowledged. Reviews by Drs. G. Ohring (NOAA/NESDIS), J. Price (USDA), D. Hastings (NOAA/NGDC), and three anonymous reviewers are appreciated. Comments by Dr. L. Stowe (NOAA/NESDIS) on the processing structure and nomenclature are appreciated. This work was prepared for publication when one of the authors (A.I.) held National Research Council Associateship at the Satellite Research Laboratory, NOAA/NESDIS, on leave from the Marine Hydrophysics Institute, Sevastopol, Ukraine.

Appendix: Frequently used acronyms and notations

AVHRR	Advanced Very High Resolution Radiometer
BRDF	Bidirectional reflectance distribution function
GAC	Global area coverage
GEWEX	Global Energy and Water Cycle Experiment
GIMMS	Global Inventory Monitoring and Modeling Studies (at NASA)
GVI	Global vegetation index (dataset)
Ch1, Ch2	Counts in channels 1 and 2 of AVHRR
δ_v	Standardized anomaly of variable V
IGBP	International Geosphere–Biosphere Programme
ISLSCP	International Satellite Land Surface Climatology Project
IR	Infrared
LST	Land surface temperature
LAI	Leaf area index
NASA	National Aeronautics and Space Administration
NDVI	Normalized difference vegetation index
NESDIS	National Environmental Satellite Data and Information Service
NOAA	National Oceanic and Atmospheric Administration
PWI	Precipitable water index
QC	Quality/cloud flag
REAF	Regional empirical angular function
ρ_1, ρ_2	Channel 1 (visible) and 2 (near IR) bidirectional reflectances
T_4, T_5	Channel 4 and 5 brightness temperatures
TOA	Top of atmosphere

$X.Y/TS$

$X = 1, 2, 3$

(1—orbital, 2—daily maps, 3—composite maps)

$Y = 1, 2, 3, 4, 5$

(1—calibrated, 2—QC flag appended, 3—atmospherically corrected, 4—surface BRDF-corrected, 5—transformed into geophysical parameter)

TS mnemonics: T —timescale, S —spatial scale

References

- Arino, O., G. Dedieu, and P. Y. Deschamps, 1992: Determination of land surface spectral reflectances using Meteosat and NOAA/AVHRR shortwave channel data. *Int. J. Remote Sens.*, **13**, 2264–2287.
- Ba, B. M., P.-Y. Deschamps, and R. Frouin, 1995: Error reduction in NOAA satellite monitoring of the land surface vegetation during FIFE. *J. Geophys. Res.*, in press.
- Carlson, T. N., E. M. Perry, and T. J. Schmugge, 1990: Remote estimation of soil moisture availability and fractional vegetation cover for agricultural fields. *Agric. For. Meteorol.*, **52**, 45–69.
- Choudhury, B. J., 1989: Estimating evaporation and carbon assimilation using infrared temperature data: Vistas in modeling. *Theory and Application of Remote Sensing*, G. Asrar, Ed., Wiley, 628–690.
- Cihlar, J., L. St.-Laurent, and J. A. Dyer, 1991: Relation between the normalized difference vegetation index and ecological variables. *Remote Sens. Environ.*, **35**, 279–298.
- , D. Manak, and N. Voisin, 1994: AVHRR bidirectional reflectance effects and composite. *Remote Sens. Environ.*, **48**, 77–88.
- Curran, P., 1980: Multispectral remote sensing of vegetation amount. *Prog. Phys. Geogr.*, **4**, 315–341.
- Dalu, G., 1986: Satellite remote sensing of atmospheric water vapor. *Int. J. Remote Sens.*, **11**, 369–393.
- Eck, T. F., and B. N. Holben, 1994: AVHRR split window temperature differences and total precipitable water over land surfaces. *Int. J. Remote Sens.*, **15**, 567–582.
- Fiedl, M. A., and F. W. Davis, 1994: Sources of variation in radiometric surface temperature over a tallgrass prairie. *Remote Sens. Environ.*, **48**, 1–17.
- Gallo, K. P., and T. K. Flesch, 1989: Large area crop monitoring with the NOAA AVHRR: Estimating the silking stage of corn development. *Remote Sens. Environ.*, **27**, 73–80.
- Goward, S. N., D. G. Dye, S. Turner, and J. Yang, 1993: Objective assessment of the NOAA Global Vegetation Index Data Product. *Int. J. Remote Sens.*, **14**, 3365–3394.
- Gutman, G., 1990: Review of the workshop on the “Use of Satellite-Derived Vegetation Indices on Weather and Climate Prediction Models.” *Bull. Amer. Meteor. Soc.*, **71**, 1458–1463.
- , 1991: Vegetation indices from AVHRR: An update and future prospects. *Remote Sens. Environ.*, **35**, 121–136.
- , 1994a: Global data on land surface parameters from NOAA AVHRR for use in numerical climate models. *J. Climate*, **7**, 669–680.
- , 1994b: Normalization of multi-annual global AVHRR reflectance data over land surfaces to common sun-target-sensor geometry. *Adv. Space Res.*, **14**, (1)121–(1)124.

- , —, and S. Olson, 1994: Towards better quality of AVHRR composite images over land: Reduction of cloud contamination. *Remote Sens. Environ.*, **50**, 134–148.
- , and A. Ignatov, 1995: Global land monitoring from AVHRR: Potential and limitations. *Int. J. Remote Sens.*, in press.
- Hastings, D. A., and L. Di, 1994: Modeling of global change phenomena with GIS using the global change data base. Part II: Prototype synthesis of the AVHRR-based vegetation index from terrestrial data. *Remote Sens. Environ.*, **49**, 13–24.
- IGBP, 1992: Improved global data for land applications: A proposal for a new high resolution data set. Global Change, Report 20, 87 pp.
- James, M. E., and S. N. V. Kalluri, 1994: The Pathfinder AVHRR land data set: An improved coarse resolution data set for terrestrial monitoring. *Int. J. Remote Sens.*, **15**, 3347–3363.
- Justice, C. O., J. R. G. Townshend, B. N. Holben, and C. J. Tucker, 1985: Analysis of the phenology of global vegetation using meteorological satellite data. *Int. J. Remote Sens.*, **8**, 1271–1318.
- , T. Eck, D. Tanré, and B. N. Holben, 1991: The effect of water vapor on the normalized difference vegetation index derived for the Sahelian region from NOAA AVHRR data. *Int. J. Remote Sens.*, **12**, 1165–1187.
- Kaufman, Y. J., and B. N. Holben, 1993: Calibration of AVHRR visible and near-IR bands by atmospheric scattering, ocean glint and desert reflection. *Int. J. Remote Sens.*, **14**, 21–52.
- Kerr, Y. H., J.-P. Lagouarde, and J. Imberton, 1992: Accurate land surface temperature retrieval from AVHRR data with use of an improved split window algorithm. *Remote Sens. Environ.*, **41**, 197–209.
- Kidwell, K., 1994: *Global Vegetation Index User's Guide*. U.S. Dept. of Commerce, NOAA/National Environmental Satellite Data and Information Service, National Climatic Data Center, Satellite Data Services Division, 126 pp.
- , 1995: *Polar Orbiter Data User's Guide*. U.S. Dept. of Commerce, NOAA/National Environmental Satellite Data and Information Service, National Climatic Data Center, Satellite Data Services Division, 410 pp.
- Kogan, F. N., 1990: Remote sensing of weather impacts on vegetation in non-homogeneous areas. *Int. J. Remote Sens.*, **11**, 1405–1419.
- Kustas, W. P., E. M. Perry, P. C. Doraiswamy, and M. S. Moran, 1994: Using satellite remote sensing to extrapolate evapotranspiration estimates in time and space over a semiarid rangeland basin. *Remote Sens. Environ.*, **49**, 275–286.
- Laszlo, I., H. Jacobowitz, and A. Gruber, 1988: The relative merits of narrowband channels for estimating broadband albedos. *J. Atmos. Oceanic Technol.*, **5**, 757–773.
- Li, Z.-L., and F. Becker, 1993: Feasibility of land surface temperature and emissivity determination from AVHRR data. *Remote Sens. Environ.*, **43**, 67–85.
- Los, S. O., C. O. Justice, and C. J. Tucker, 1994: A global $1^\circ \times 1^\circ$ NDVI dataset for climate studies derived from the GIMMS continental NDVI data. *Int. J. Remote Sens.*, **15**, 3493–3518.
- Malingreau, J.-P., 1986: Global vegetation dynamics: Satellite observations over Asia. *Int. J. Remote Sens.*, **7**, 1121–1146.
- Mintz, I., and D. Walker, 1990: Land surface energy and water budgets derived with NDVI. *Proc. Workshop on the "Use of Satellite-Derived Vegetation Indices in Weather and Climate Prediction Models"*, Camp Springs, MD, NESDIS, NMC, 113 pp.
- Nemani, R., L. Pierce, S. Running, and S. Goward, 1993: Developing satellite-derived estimates of surface moisture status. *J. Appl. Meteor.*, **32**, 548–557.
- Ohring, G., and J. C. Dodge, 1992: The NOAA/NASA Pathfinder. *IRS '92: Current Problems in Atmospheric Radiation*, S. Keavallik and O. Kärner, Eds., A. Deepak, 405–408.
- Pinty, B., and M. M. Verstraete, 1992: On the design and validation of surface bidirectional reflectance and albedo models. *Remote Sens. Environ.*, **41**, 155–167.
- Prata, A. J., 1993: Land surface temperature derived from the Advanced Very High Resolution Radiometer and the Along-Track Scanning Radiometer. 1. Theory. *J. Geophys. Res.*, **98**, 16 689–16 702.
- Price, J. C., 1990: Using spatial context in satellite data to infer regional scale evapotranspiration. *IEEE Trans. Geosci. Remote Sens.*, **28**, 940–948.
- , 1991: Timing of NOAA afternoon passes. *Int. J. Remote Sens.*, **12**, 193–198.
- Rao, C. R. N., 1993: Nonlinearity corrections for the thermal infrared channels of the Advanced Very High Resolution Radiometer: Assessment and recommendations for corrections. NOAA Tech. Rep. 69, U.S. Dept. of Commerce, 25 pp.
- , and J. Chen, 1994: Post-launch calibration of the visible and near IR channels of AVHRR on NOAA-7, -9, and -11 spacecraft. NOAA Tech. Rep. NESDIS 78, U.S. Dept. of Commerce, 22 pp.
- Rossow, W. B., and R. A. Schiffer, 1991: ISCCP cloud data products. *Bull. Amer. Meteor. Soc.*, **72**, 2–20.
- Roujean, J. L., M. Leroy, A. Podaire, and P. Y. Deschamps, 1992: Evidence of surface reflectance bidirectional effects from a NOAA/AVHRR multi-temporal data set. *Int. J. Remote Sens.*, **13**, 685–698.
- Rouse, J. W., R. H. Haas, J. A. Schell, and D. W. Deering, 1973: Monitoring vegetation systems in the Great Plains with ERTS. *Proc. Third ERTS Symp.*, Washington, D.C., NASA SP-351, 309–317.
- Sellers, P., 1985: Canopy reflectance, photosynthesis, and transpiration. *Int. J. Remote Sens.*, **7**, 1251–1262.
- Stowe, L. L., R. M. Carey, and P. P. Pelegrino, 1992: Monitoring the Mt. Pinatubo aerosol layer with NOAA-11 AVHRR data. *Geophys. Res. Lett.*, **19**, 159–162.
- Tanré, D., B. N. Holben, and Y. J. Kaufman, 1992: Atmospheric correction algorithm for NOAA-AVHRR products: Theory and application. *IEEE Trans. Geosci. Remote Sens.*, **30**, 231–248.
- Tarpley, J. D., 1991: The NOAA Global Vegetation Index product—A review. *Palaeogeogr., Palaeoclimatol., Palaeoecol.* (Global and Planetary Change Section), **90**, 189–194.
- , S. R. Schneider, and R. L. Money, 1984: Global vegetation indices from NOAA-7 meteorological satellite. *J. Climate Appl. Meteor.*, **23**, 491–494.
- Tateishi, R., and K. Kajiwara, 1991: Land cover monitoring in Asia by NOAA GVI data. *Geocarto Int.*, **4**, 53–64.
- Thomas, G., and A. Henderson-Sellers, 1987: Evaluation of satellite derived land cover characteristics for global climate modelling. *Clim. Change*, **11**, 313–347.
- Townshend, J. R. G., C. O. Justice, and V. Kalb, 1987: Characterization and classification of South American land cover types using satellite data. *Int. J. Remote Sens.*, **8**, 1189–1207.
- Tucker, C. J., 1979: Red and photographic infrared linear combinations for monitoring vegetation. *Remote Sens. Environ.*, **8**, 127–150.
- , J. R. G. Townshend, and T. E. Goff, 1985: African land-cover classification using satellite data. *Science*, **227**, 369–375.
- , W. W., Newcomb, S. O. Los, and S. D. Prince, 1991: Mean and inter-year variation of growing season normalized difference vegetation index for the Sahel 1981–1989. *Int. J. Remote Sens.*, **12**, 1133–1135.
- Tuller, S. E., 1968: World distribution of mean monthly and annual precipitable water. *Mon. Wea. Rev.*, **96**, 785–797.